1.1 Perovskites: Structural Diversity

The first natural perovskite, $CaTiO_3$ was discovered by German chemist and mineralogist Gaustav Rose in 1839; which is known as perovskite on the name of Lev Alexeievitch Perovsky [1]. The general chemical formula belongs to this family is termed as ABX_3; where A and B are cations and X is the anion either oxygen or halide group elements. The valence of A and B is taken to be in such a way that it could be compensated by the charge of anions. Majority of elements combined in the form of (A^{3+} - B^{3+}), (A^{2+}, B^{4+}), (A^{+}, B^{5+}) from periodic table is found to be exhibit perovskite structures, e.g. $LaAlO_3$, $BaSnO_3$, $KNbO_3$ etc. The perovskite structure can be described in the framework of BO_6 octahedra; which is formed by the sharing of oxygen present at the corner. In this structure the A atom is situated at the corner position of the cube and shared by eight octahedra, while B is situated at the body centred position of the cube and oxygen is present at the face of each cubic face and forms an octahedra by B-cation, as seen from Figure 1.1. The perovskite structure can also be understood in terms of AO rock salt layer interconnecting by two layers of BO_2 from above and below in order to describe the layer structure. The perovskite structure is one of the highest multifunctional structures in which an incredibly wide range of phases can be produced with completely different functions through structural manipulation [2].

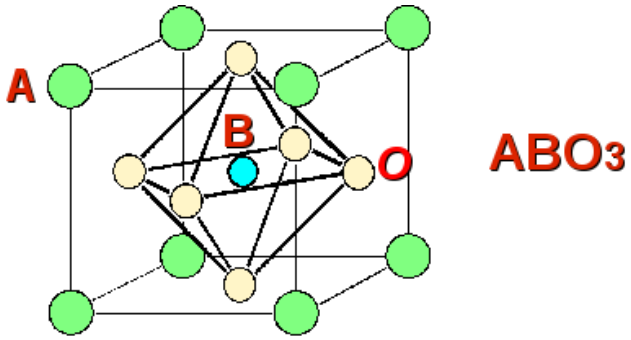

Figure 1.1 A unit cell of ABO_3 type cubic perovskite oxide structure.

Due to the extreme flexibility of structures by replacing cation, one dimension of the compositional and structural diversity in perovskite can be sustained by the distortion created by the cation. The degree of mismatch between the layer of AO and BO_2 (determined by mismatch in ionic radii) determines the tolerance of perovskite structure [3]. The perfect geometrical match between AO and BO_2 layers give an ideal perovskite structure. Geometrically consistency is determined by the equation given as follows:

$$r\,(A-O) = \sqrt{2}\,r\,(B-O) \qquad (1.1)$$

Where, $r\,(A-O)$ and $r\,(B-O)$ are the distances obtained from ionic radii of the respective atom. The persistence of structure is usually expressed in terms of the "**Tolerance Factor** (**t**)". It was first introduced by Goldschmidt, which can be expressed mathematically as follow [3];

$$t = \frac{r_A + r_O}{\sqrt{2}\,(r_B + r_O)} \qquad (1.2)$$

Where, r_A, r_B and r_O are the ionic radii of cation A, B and anion O respectively. Depending on the tolerance factor various crystal structures are possible, for example t=1 gives an ideal cubic structure. The other crystal structures and their tolerance factor are given in Table 1.1.

Table 1.1 Tolerance factor of different crystal structure.

Goldschmidt tolerance factor (t)	**Structure**	**Explanation**	**Example**
>1.0	Hexagonal or Tetragonal	A ion too big or B ion too small.	$BaTiO_3$[4]
0.90-1.00	Cubic	A and B ions have ideal size.	$BaSnO_3$ [4] $BaTiO_3$ [5]
0.71 - 0.90	Orthorhombic/Rhombohedral	A ions too small to fit into B ion interstices.	$GdFeO_3$ [4] $CaTiO_3$ [4,6]
<0.71	Triclinic/Monoclinic	A ions and B have similar ionic radii.	Ilmenite, $FeTiO_3$ [7]

Consider an example $t = 1.002$ approaches ideal cubic structure of $BaSnO_3$ with space group $Pm\bar{3}m$. However, the variety in the perovskite structure exhibited for lower symmetry which leads for lower t as 0.8. The perovskite have $A - O$ bond under tension and $B - O$ bond under compression for $t < 1$. In order to reduce this effect, the oxygen shared corner BO_6 octahedral consistently tilt or rotate about pseudo cubic axis which accommodate smaller size of cations A in the interstices space between them [3]. Tilting in the octahedral reduces the $Pm\bar{3}m$ symmetry to lower symmetry subgroups. Using crystallographic principle, this particular tilt in octahedra is associated with specific subgroup or class of symmetry [7–9]. In addition, the rotation of octahedral or distortion it leads to a change in the bond length of $B - O$ due to John-Teller distortion. The John-teller distortion has active because the cation B is belongs to the Transition metal such as Mn^{3+}, Fe^{4+}, Ni^{3+}, Cu^{2+} etc. In transition metal, each element have unpaired electron in their d shell [10, 11]. If t > 1, the A cations are too large to fit within the polyhedral framework of the BO6 at the 12 fold site and the hexagonal polytype structure can be formed. Of particular interest related with stability of the cubic phase in $BaTiO_3$ with tolerance factor $t \approx 1.04$. Such a high tolerance factor induced a cooperative ferroelectric displacement of Ti^{4+} cations [12]. Due to presence of lone pair electrons in cations which have ns^2 core electron induced special structural effects resulted ferroelectricity. Due to steriochemical lone pair effect of Pb ions on the oxygen framework of $PbTiO_3$, it results a strong displacement of Pb^{2+} and Ti^{4+} ions from their polyhedral centres [13]. Another variant of structural diversity in stoichiometric perovskites is provided by cation ordering on either A or B - sites.

1.2 Properties of Perovskites

It is useful to study various properties like electrical properties, magnetic properties and optical properties based on the variety of structure present in the perovskites. These properties could be improved either by substitution of dopant or by changing the processing parameters like time temperature etc. The properties of perovskites can be modified by compositional modification also; in case of compositional modification there are three types of substitution [14]. These types of substitution are discussed below;

Isovalent Substitution: In this substitution, the substituent ion has the same valency as host ion. This type of substitution may be done at either A-site, B-site or both site of ABO_3. Therefore, no excess charge is generated by this substitution and the material becomes overall neutral. For example Ba^{2+} at Sr^{2+} site in $SrSnO_3$, Ti^{4+} at Sn^{4+} site in $SrSnO_3$ and so on.

Hetrovalent Substitution: In this case, the valency of the substituent ion is different from host ion. This type of substitution can also be done either at A-site, B-site or both sites. There are two types of substitutions in this category;

(i). Acceptor type substitution: In this category, the substituent ion has lower valency than host ion, leading creation of excess hole or charged vacancy in the unit cell. For example, Eu^{3+} at Sn-site of $SrSnO_3$ where the following charge compensation mechanism takes place.

$$Eu_2O_3 \xrightarrow{SrSnO_3} 2Eu_{Sn}{}' + Sr_{Sr}^{x} + 3O_0{}^{x} \qquad (1.3)$$

$2Eu_{Sn}{}'$ = The excess charge on a lattice is compensated by either creation of a hole or oxygen vacancies, $2Eu_{Sn}{}' = [2h^{\cdot}] = [V_{\ddot{O}}]$

(ii). Donor type substitution: In this class of substitution, the substituent ion has higher valency than host ion, which leads the creation of excess charge in the unit cell. For example, La^{3+}, Nd^{3+} at the Sr-site of $SrSnO_3$, the charge compensation mechanism takes place as follows:

$$La_2O_3 \xrightarrow{SrSnO_3} 2La_{Sr}^{\cdot} + Sn_{Sn}^{x} + 3{O_0}^{x} \quad (1.4)$$

Where, $2La_{Sr}^{\cdot}$ = is the excess charge on the lattice which has been compensated by either creation of electron or cationic vacancies, $[2La_{Sr}^{\cdot}] = [2e'] = [V_{Sr}'']$

Valence compensated substitution: Simultaneous substitution of a combination of hetrovalent ions at A and B sites in ABO_3, results in excess of charge carrier in the unit cell. The resultant charges carrier in the unit cell is compensated by internal charge compensation mechanisms.

Based on the above compositional modification and charge compensation processes the properties of perovskite oxides have been modified and discussed as below;

Electrical properties

Generally, the synthesis of the ceramic oxides (ABO_3) has been carried out at high temperature, i.e., $\leq 1400^oC$, and at this much high temperature the loss of oxygen takes place from the lattice site which makes the site positively charged. This positively charged site maintained the charge neutrality by reduction of cation B or creation of electron which makes ABO_3 as oxygen deficient phase [14]. The presence of oxygen vacancy manipulates the oxidation state of transition metal or post transition metals. The manipulation of valance states of transition metal improved the electronic as well as ionic conductivity depending on the types of substitution [15–17]. Most of the perovskites served as a good oxygen ion conductor, applicable in various electrochemical devices such as solid oxide fuel cells (SOFCs) [16, 17]. Rare earth (RE)

based aluminates ($LnAlO_3$) doped with acceptor attracted the most significant interest since 1970 [18, 19], due to their low cost, bearable thermal expansion coefficient and higher stability with respect to volatilation compared to doped $CeO_{2-\delta}$ and $LaGaO_{3-\delta}$ [20–23]. The maximum oxygen ion conductivity and minimum vacancy enthalpy association is improved by incorporating Sr^{2+} at the Ln site and Mg at Al site of $LnAlO_3$ site, which was approximately 0.7 Scm^{-1} [22].

Piezoelectric effect is the second interesting properties in which the electric charge is created by applying pressure. It also exhibited an excellent electromechanical properties near to the morphotrophic phase boundary (MPB) compositions [23–26]. The $PbZrTiO_3$ (PZT) is the most common piezoelectric ceramic materials which were used from last decades [24]. Ultimately, replacing of Pb-based materials is required due to environmental and toxicity issues related with lead. Therefore, extensive studies have been reported on the lead free materials including perovskites such as $(Na_{0.5}Bi_{0.5})TiO_3$ (NBT) and $(K_{0.5}Na_{0.5})NbO_3$ (KNN) and their solid solutions [25–30]. KNN has the piezoelectric coefficient (d_{33}) of the order of ≈ 100 pC/N [25]. With the addition of different perovskites such as $LiTaO_3$, $LiNbO_3$, $LiSbO_3$ and $SrTiO_3$ in KNN based materials; it was showing soft piezoelectric behaviour which is analogous to donor doped PZT materials. Using conventional solid state reaction for the synthesis of KNN modified materials achieved nearly full densification [25, 31, 32].

In Multilayer ceramics capacitors, Barium Titanates ($BaTiO_3$) perovskite are frequently used as high permittivity dielectrics [33, 34]. Alkaline earth titanates such as $CaTiO_3$, $SrTiO_3$ and $BaTiO_3$ etc. have been also studied extensively for technological applications in primary science as well as electronic devices due to its exciting electrical properties, structural behaviour and chemical stability. The high dielectric constant in $BaTiO_3$ ceramics results due to transition in their crystal structure from cubic to

tetragonal. In $BaTiO_3$ ceramic, the temperature was a substantial factor which affects the crystal structure and polarization characteristics of $BaTiO_3$ [35]. The $BaTiO_3$ has possessed a spontaneous polarization at room temperature due to the presence of non-centrosymmetry in the centre of oxygen octahedron [36]. As the temperature increases, the thermal vibration in $BaTiO_3$ results in the random orientation of titanium ions to the octahedral interstitial position. The dielectric properties are also enhanced by making the solid solution of two phases like ferroelectric $BaTiO_3$ and non - ferroelectric $BaSnO_3$, in which the replacement of Sn^{4+} ion on the Ti^{4+} site results a shift of Curie temperature. Due to shift in curie temperature, a high dielectric constant value was obtained because of the presence of different conductive regions which produced a chemical microheterogeneity at the level of nano-polar regions (Random occupation of Sn^{4+}, Sn^{2+} at Sn-site and Ti^{4+}, Ti^{2+} at Ti-site) [37].

Magnetic Properties

The perovskites compounds also shows interesting magnetic properties [38–42]. Among them the $LaMnO_3$ showed versatile magnetic properties at liquid air temperature while the other perovskites like $LaCrO_3$ and $LaFeO_3$ are not [40, 41, 43, 44]. It appeared that $LaMnO_3$ was ferromagnetic at liquid air temperature only when it contains partial fraction of manganese ion like higher valence state as well as lower valence state than Mn^{3+}. The manipulation of valance state is also performed by treating $LaMnO_3$ at high temperature in presence of oxygen rich atmosphere. In this process, the formation of oxygen vacancy takes place in sample and electron associated with oxygen vacancy compensate the overall charge neutrality, which can be used in manipulation of the valence state of Mn. The partial substitution of alkaline earth element at La site and higher valence atom at Mn-site like $La^{3+}Mn^{3+}O_3^{2-}$ - $Me^{2+}Mn^{4+}O_3^{2-}$ (Me^{2+} larger divalent ions) is another manipulative method [45]. These methodology is tried for investigating

the binary system such as $LaMnO_3$-$CaMnO_3$, $LaMnO_3$-$SrMnO_3$, $LaMnO_3$-$BaMnO_3$, $LaMnO_3$-$CdMnO_3$, $LaMnO_3$-$PbMnO_3$ [42–44]. In all these systems, at least over a certain compositions, ferromagnetic mixed crystal was formed. The ferromagnetism of hole doped specimen is explained by double exchange interaction taking place between Mn^{3+} and Mn^{4+} ions [42, 44]. The magnetic properties can be modified in non-magnetic perovskites by incorporating small amount of magnetic ion or rare earth elements also known as dilute magnetic semiconductor (DMS) [45]. The various rare earth doped ion into BaTiO3, $BaSnO_3$, $LaMnO_3$, $LaAlO_3$ etc. have been widely investigated for spintronic applications [45, 46]. In case of rare earth element doping, the magnetism can be explained in terms of direct interaction, exchange interaction and bound magnetic polaron (BMP) model [47, 48].

Optical Properties

The invention of a white light emitting diode (LED) has brought revolution to this century's lighting technology that suppressed the conventional use of incandescent or fluorescent lamps. They have excellent properties such as high brightness, cost reliable, low power consumption and long service life [49, 50]. Rare earth (RE) doped phosphors material have found important applications in the development of white LEDs [51]. The perovskite structure ($A^{2+}B^{4+}O^{2-}$) doped with activators (Er^{3+}, Yb^{3+}) have become significant importance because of their easily tunability of emission properties found in different regions [52]. These perovskite oxides form very stable matrices, both chemically/physically and also capable to work in different environments. Particularly, in the field of solid state lighting these oxides based phosphors become a potential candidate in the area of field emission display (FEDs) and plasma panel display (PDPs) devices [53]. The luminescence properties of perovskite oxide based phosphors having structure such as $A^{2+}B^{4+}O^{2-}$ (A: Ca, Sr, Ba and B: Sn, Ti, Zr, Si, Hf, etc.) activated with

different rare earth ions including Sm^{3+}, Tm^{3+}, Pr^{3+}, Eu^{3+}, Tb^{3+}. The orange, red, green, yellow and red-orange emissions were extensively studied [54–56].

Recently, the transparent and conductive oxides (TCO) with the perovskite structure were explored extensively by ionic substitution and carrier doping. The thin films of In, Sb, La-doped $SrTiO_3$, Nb-doped $CaTiO_3$, and Cd_3TeO_6 have been extensively studied for TCO application [57]. The thin film of La and Sb-doped $BaSnO_3$ deposited on the substrate of $SrTiO_3$ (001) (STO) using laser ablation method are found that these films show not only the good stability but also high conductivity and good optical transparency in the visible region. Moreover, the growth parameters for these films are compatible with the films of other perovskite such as ferroelectric (Pb, Zr)TiO_3. The TCO films of these materials can be used as a potential candidate for optoelectronic device applications especially based on perovskite heterostructures [58].

1.3 Applications of Perovskites

Thus one can conclude that the perovskite type structures are the most stable structure. The perovskites are studied extensively and tried for various kinds of application dependent on the modification in perovskite oxides. The undoped /rare earth or transition metal modified $LnMnO_3$ perovskites are found as a potential candidate in the application of electrolyte [59], cathode and anode materials for solid oxide fuel cell [60]. $A^{2+}B^{4+}O_3^{2-}$ type perovskites structure are used for sensor applications to senses different gas like ethanol, hydrogen, oxygen, nitrogen, ammonia etc. [61]. The modified perovskite type structures $AA'BB'O_{3-\delta}$ (A = Ln Lanthanides, A' = Alkaline earth metal, B = Transition metal/Alkali metal B' = Rare earth element, those have valance state other than cation B) have been used in application of electronic ceramics [62], superconductors [63], and solid state lighting [64]. Alkaline earth elements based

titanates ($BaTiO_3$) is extensively used as ferroelectric as well as piezoelectric materials due to their tetragonal crystal structure. Further modification made by rare earth element and transition metal in $BaTiO_3$, it can be used in spintronics and phosphor application for imaging purposes [65, 66]. However, rare earth modified $SrTiO_3$ was used as electrode materials (Cathode/anode) in solid oxide fuel cell, Sm^{3+} modification gives better luminescence in the intense emission in orange region and Eu^{3+} modification results intense red orange emission [67]. Although, the alkaline earth stannates ($BaSnO_3$) is found as a wide band gap semiconductor at room temperature and modification by rare earth and transition metal it can be used for electrode materials in solid oxide fuel cell (SOFC), electrode material for Dye Sensitized Solar Cell [68], dilute magnetic semiconductor (DMS) [45], magnetic memory devices [69]. Even though it can be further transforms to conductor by changing the processing parameters and doping concentration [61]. The perovskite not only in individuals but also their solid solution can be used in dielectric chip, thermal stable capacitor, barrier layer capacitor, memory devices and so on [66–68].

Therefore, it can be concluded that it can be used in multiple applications based on variation in processing parameters, change in doping and their concentrations, structural transitions, and charge compensation mechanism.

1.4 Ruddlesden D Popper (RP) Oxide Phase

High tolerance of the perovskite structure into low dimensionality gives a second dimension structural diversity in perovskite. In terms of the layered representation of perovskite structure (Figure 1.1), the parent structure of perovskite phase is consists of alternate stacking of AO and BO_2 layers. The flexibility of these structures means that this stack can be interrupted by intergrowth entities and flexible to accommodate

various types of intergrowth of dopants (in terms of being off set in position and sequence). These results are interesting which occurred in several homologous series and structural families. These structures are collectively referred as layered perovskite. Ruddlesden Popper, Dion–Jacobson, Aurivillius phases and the huge family of high temperatures superconducting cuperates [73] are the examples of layered perovskite. The Ruddlesden Popper (RP) series is an important and basic example of layered perovskite in which the alternate stacking of AO-BO_2 is interrupted by additional layer of AO. Hence, the Ruddlesden Popper oxide can be gernalized to an expression $AO(AO\text{-}BO_2)_n$ or $A_{n+1}B_nO_{3n+1}$, for example n=1 A_2BO_4, n=2 $A_3B_2O_7$ and so on as shown in Figure 1.2. The general chemical formula of n=1 member of the RP series is A_2BO_4 and its structure is well known as K_2NiF_4 type structure. In Dion-Jacobson and Aurivillius phases [73] materials, the perovskite layer stack is interrupted by intergrowths containing M^{1+} (usually alkali metal) and M^{3+} ions respectively. However, Layered cuperates [74] shows greater flexibility of the AO and BO_2 (CuO_2) layers to accommodate more than one type of intergrowth layers. Three types of intergrowth layers often occur in layered cuperates: M (Na, K), MO (i.e TiO, BaO, BiO). The Ruddlesden Popper phase compounds of this family and their different possible compositions of compound giving special attention in structural diversity, due to their potential impact on industrial applications.

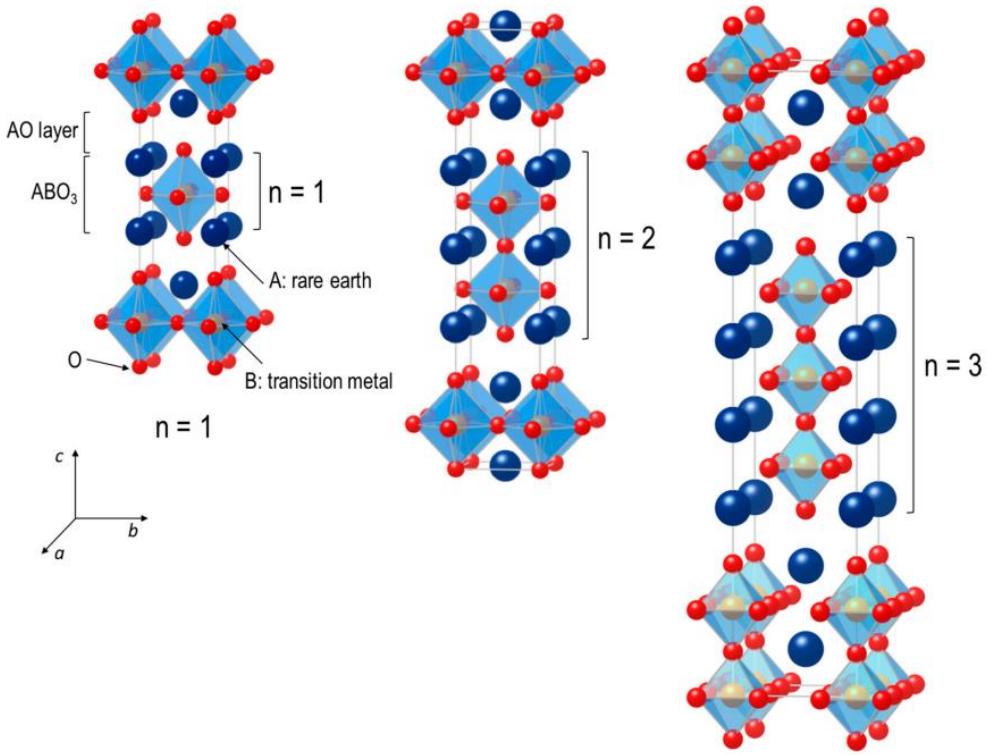

Figure 1.2 Schematic crystal structures of n = 1, 2 and 3 members of Ruddlesden–Popper type $A_{n+1}B_nO_{3n+1}$ [75]**.**

1.5 Structure of Ruddlesden Popper Phase

As already discussed above that the Ruddlesden Popper oxide phase A_2BO_4 consist two different kind of layers i.e., a rock salt layer AO interconnected with a perovskite ABO_3 along c-direction. A_2BO_4 type's structure exhibits anisotropic features due to their arrangements of atoms in unit cell. Generally, in these materials A-site cations are rare earth element or alkali metal and B-site cations are transition metal or post transition metal. Figure 1.3 shows a unit cell of A_2BO_4 type structure with A-O_9 and B-O_6 arrangement of atoms. The complex oxides A_2BO_4 crystallized into K_2NiF_4 type structure. In this structure the perovskite slabs of unit thickness stacked one over the rock salt layer along the c-axis, such that the adjacent slabs are displaced relative to one another by $\left(\frac{1}{2},\frac{1}{2},\frac{1}{2}\right)$ [76].

For K_2NiF_4-type structure, the structure of RP oxides A_2BO_4 is remains stable only for those elements whose ratio r_A/r_B lies in between 1.7 and 2.4 [77]. According to the literature survey, for all the known compounds, only 5% have the values of r_A/r_B lies outside the prescribed range. Poix has calculated the relation among the average cation-oxygen distances associated to the 9 and 6 coordinated sites (φ_A and β_B) and volume V of the unit cell using invariant method in K_2NiF_4 structure [76] :

$$0.99615\, V^{1/3} = \beta_B + \varphi_A 2^{1/2} \qquad (1.5)$$

K_2NiF_4-type structure is a two-dimensional array in which the equatorial anions of BO_6 octahedra are only linked through the corners (Figure 1.3). Recently, a new relation on the tolerance factor has been formulated for the Nd_2CuO_4-type structure by considering a geometrical matching between the bond distances. On the basis of geometrical matching in Nd_2CuO_4 structure, the tolerance factor is given by $t = \left[3\sqrt{2}r_O + \frac{2\sqrt{6}(r_A + r_O)}{9(r_B + r_O)}\right]$ where, r_A, r_B and r_O are the ionic radii of A, B and O ions, respectively. Based on the values of tolerance factor different phases of Nd_2CuO_4 structures are possible such that T' phases occur if tolerance factor t < 1.00, while T phases occurred for tolerance factor t > 1.00. The T^* phase of Nd_2CuO_4 is exists in a very narrow region between the stability boundaries of the other two structure T and T' types [78].

The three-dimensional character increases in higher members of the family because of presence of increased numbers of ABO_3 slabs. In these structures, the A-site cation has a coordination number of 9 locating at the boundary between the two of layers, while B-site cations are positioned at the centre of octahedron formed by six oxygen anions. The length of bond B-O is different due to arrangement of two kinds of oxygen species in BO_6 octahedra which are referred as “apical” and “equatorial” oxygen, along a=b-

direction and c-direction respectively. The BO_6 octahedral corners share with each other, extending infinitely in the a, b plane, and the n units of such planes stack in the c-direction to form the perovskite slab. If A is a rare earth and/or alkaline earth ion and B is a transition metal ion / post transition element in such compounds, the electrical transport and magnetic properties of these phases within a given series are governed by ion identity valence, n perovskite slabs width, B-O-B bond angle and oxygen content. [72,73].

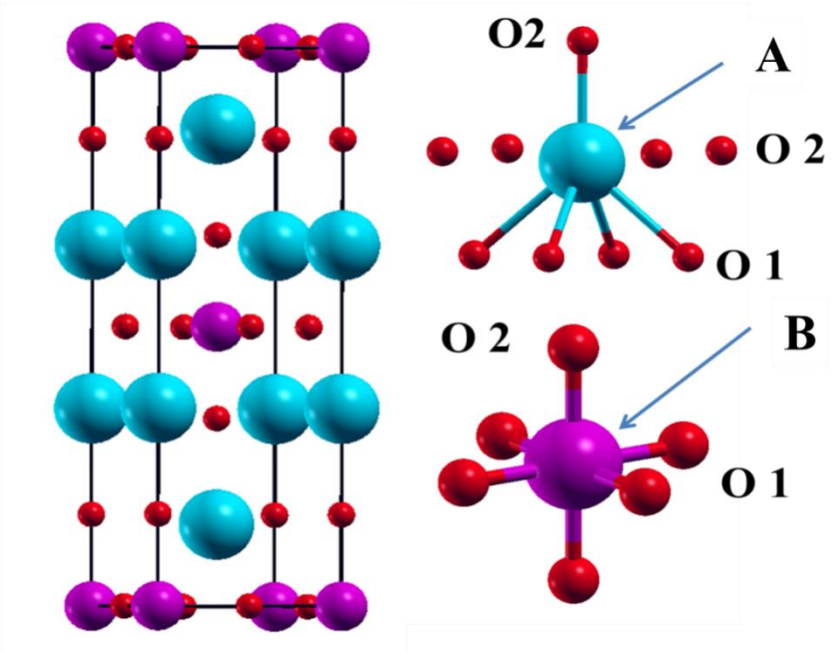

Figure 1.3 Unit cell of A_2BO_4 and arrangement of A-O_9 and B-O_6 arrangement**.**

1.6 Application of Ruddlesden Popper Phase

It is interesting to note that in many RP type compounds, magnetic properties reflect itinerant electron behaviour, while the electric transport properties do not. Even though the predominant phases of RP compounds are both insulating and metallic. The n = 1 phase of RP family shows lowest electric resistivity of the order 10^{-2} Ω-cm. Generally, the resistivity is decreases for higher members of this family because of the increasing three-dimensional character [77]. Sr_2FeO_4 has resistivity of several orders of magnitude

higher than their corresponding n = 2 member [79]. In $La_{n+1}Ni_nO_{3n+1}$ family, the room temperature resistivity (ρ_{300}) decreases from - 250 Ω-cm for the n = 2 member and l.8 Ω-cm for the n= ∞ member [78]. However, higher the members of analogous series could be exception; Sr_2VO_4 is an insulator, while $Sr_4V_3O_{9.7}$ is metallic down to 4.2 K [79–81]. Moving upwards from n = 1 to higher members of the family, an evolution in metallic conductivity is observed. The discovery of superconductivity in the $La_{2-x}Ba_xCuO_4$ system was derived from the La_2CuO_4, has added additional dimension in the investigation of these phases [72,73]. However, there was a great deal of interest in the physical and structural chemistry of perovskite - related compounds for their wide range of applications, such as ideal semiconductors, magnetic materials, high temperature superconductors, catalysts, electrode materials etc. even before the discovery of superconductivity [81, 82]. The properties of $La_2CuO_{4+\delta}$ are extremely sensitive to change in oxygen stoichiometry. An antiferromagnetic and semiconductor behavior is shown by a negative value of δ in $La_2CuO_{4+\delta}$. However, antiferromagnetism disappears with change in oxygen stoichiometry as small as 1%. As δ becomes positive, the holes are introduced into the structure and metallic behaviour is observed [76]. When La_2CuO_4 is doped with holes either by introducing excess oxygen into the structure or partial replacement of La by alkaline earth metal ions, then it oxidized the mixed valent state of Cu from Cu^{2+} to Cu^{3+} and responsible for showing superconductivity [76].

Anion related non stoichiometric is also very common in perovskite and related compounds. Low concentrations of oxygen vacancies or interstials in perovskite type oxide are often disordered and results in potential applications of material as ionic or mixed ionic electronic conductors (MIECs). However, the higher degree of oxygen deficiency results p-type semiconductor behaviour in ordered structures and improves their hole conductivity. The $La_{n+1}Ni_nO_{3n+1}$ (n= 1, 2 and 3) series is one of the widely

studied systems. The crystal structure of La_2NiO_4 is reported to be tetragonal with space group $I4/mmm$. However, X-ray diffraction (XRD) studies indicate a monoclinic distortion. The unit cells of $La_3Ni_2O_7$ and $La_4Ni_3O_{10}$ are exist in orthorhombic crystal structure which belongs to the space group $Fmmm$ [83]. The electronic transport and magnetic properties has been improved across the homologous series with increasing n, due to their interesting 3-dimensional character and percolation threshold. La_2NiO_4 exhibits a semiconductor to metal transition around 550 K, while $La_{2-x}Sr_xNiO_4$ is reported to be exhibit a superconducting state down to 70 K [77]. La_2NiO_4 annealed in CO_2 atmosphere at 1400 K, show evidence for long range antiferromagnetic ordering. $La_2NiO_{4+\delta}$ also exhibits mixed electronic and ionic conductivity which makes it useful for cathodes in IT-SOFCs, ceramic membranes for oxygen separation. The value of thermal expansion coefficients (TEC) $\approx 13.0 \times 10^{-6}$ K^{-1} for $La_2NiO_{4+\delta}$ was close to the TEC of conventional materials which are widely used as electrolytes in SOFC like $Zr_{0.92}Y_{0.08}O_{2-y}$ (YSZ), and $Ce_{0.9}Gd_{0.1}O_{2-y}$ (CGO). This is the possible reason which makes these materials more popular than other oxides and perovskite oxides [84]. The similar TECs values guarantee the thermo-mechanical compatibility between cell components. In their crystalline structure accommodation of interstitial oxygen promotes the ionic conductivity [85], and the p-type electronic conductivity [86]. Although, the value of oxygen non-stoichiometric of layered perovskite (RP phases) playing a key role in the improvement of the electronic and ionic conductivity. Most of these compounds, showing interesting electric transport and magnetic properties, crystallizes either in tetragonal or orthorhombic crystal symmetry in the space group $I4/mmm, Fmmm$ or $Cmca$ [87–90].

Magnetic studies suggest that Co^{3+} ions is present in both high − as well as in low-spin states in equal proportions of $LaSrCoO_4$, while the material undergoes a spin state

transition above than 400 K [91]. Many manganites having perovskite-related structure such as (La, Sr)$_{n+1}$Mn$_n$O$_{3n+1}$ (n =1, 2 and 3) exhibit ferromagnetism and shows insulator-metal transition at low temperature [92]. These materials also show colossal magnetoresistance (CMR) due to presence of the mixed valence state Mn^{3+}/Mn^{4+} in the manganites which creates mobile charge carriers and canting of Mn spins [92, 93].

The Ruddlesden popper oxide, A_2BO_4 are also found more promising candidates for electrochemical energy devices due to their higher oxygen surface kinetics and oxygen diffusion within the materials [75]. It can accommodate excess of oxygen within space available between the perovskite and layer, which improves oxygen surface kinetics and oxygen diffusion either by interstitialcy or via migration through the available sites of oxygen. Consequently, the electrochemical properties of A_2BO_4 type materials improved by improvement in the transport of oxygen vacancy or oxygen ion. Additionally, the different type of oxygen defects affected the valence state of transition metal as a result of change in oxygen stoichiometry and thus leads to lattice expansions different directions. The defect processes in RP oxides are dominated by anion Frankel disorder [89] and can be expressed as;

$$O_o^x \leftrightarrow V_O{}^{\cdot\cdot} + O_i'' \qquad (1.6)$$

The oxygen diffusion coefficient D_o can be expressed in terms of defect concentrations and their diffusivity as [89];

$$D_o = D_v[V_O{}^{\cdot\cdot}] + D_i[O_i''] \qquad (1.7)$$

Where D_v and D_i are the vacancy and interstitial diffusion coefficient respectively. $[V_O{}^{\cdot\cdot}]$ and $[O_i'']$ represents the concentration of oxygen vacancies and oxygen interstitials respectively.

Many layered perovskites of titanium, and niobium and their mixed analogues have been studied recently because of their possible applications in catalysis and electrochemistry [72,85,86]. There is growing interest in the proton exchange and subsequent dehydration of the layered alkali oxides. $K_2Nd_2Ti_3O_{10}$ and $Na_2Nd_2Ti_3O_{10}$ spontaneously intercalate water, and acid exchange of the compounds leads to formation of the protonated phases [88, 89].

The catalytic properties of the perovskite - type mixed oxides has effective use in various oxidation and reduction reactions, particularly depollute the exhaust gases. Many studies have shown that the catalytic performance of A_2BO_4 mixed oxides is largely associated with the A - site and B - site ions and their corresponding valences, as well as the crystal microstrain [96]. Catalytic oxidation studies of CO and C_3H_8 were reported on $LnSrBO_4$ catalysts [87,88]. On the other hand, the catalytic reduction of NO and NO + CO over $LnSrBO_4$ catalysts have also been studied [97].

1.7 A_2BO_4 Structure Based Layered Perovskite

The K_2NiF_4 type mixed oxides with A_2BO_4 structure which consist of alternating layers of ABO_3 perovskite and AO rock salt, recently have been studied as new materials due to their low cost, high catalytic activity and high thermal stability [98]. Replacing A- and/or B - site cations with other metal cations often lead to formation of crystal microstrain. This type of structure forms solid solutions with many cations, enabling a wide range of changes in physical and chemical properties.

Based on the different types of doping at either A/B or both sites, the oxygen non stoichiometry δ in $A_2BO_{4\pm\delta}$ can be varied, and in order to compensate the lack of overall charges created by this δ is to be compensated by the further manipulation in valence states of multivalent ions B. The advantage of this type of crystal structure mainly

A_2BO_4 types is accommodation of excess oxygen ion in space between the perovskite ABO_3 and layer AO. However, in case of ABO_3 perovskite due to their compact structure it can be only form oxygen deficient structure like $ABO_{3-\delta}$ ($LaAlO_{3-\delta}$, $BaSnO_{3-\delta}$, etc.). The formation of oxygen interstitial in ($A^{3+}{}_2B^{2+}O^{2-}{}_4$) can be understood by following equation;

$$O_O \rightarrow O_i'' + 2h^{\cdot} \qquad (1.8)$$

The creation of hole oxidize the valence states from lower valence state to higher valence state which can be shown by following equation to compensate the overall charge created by this defective oxygen;

$$B^{2+} + 2h^{\cdot} \rightarrow B^{4+} \qquad (1.9)$$

Moreover, the loss of oxygen in ($A^{2+}B^{4+}O^{2-}{}_4$) can be understood by following equation;

$$O_o \rightarrow \frac{1}{2}O_2(g) + V_{\ddot{O}} + 2e' \qquad (1.10)$$

The creation of electron in oxygen loss process reduces the valence state of multivalent ion to compensate the overall charge created by oxygen vacancy which can be understood in terms of equation (1.11);

$$B^{4+} + 2e' \rightarrow B^{2+} \qquad (1.11)$$

Based on the above charge compensation mechanism the properties of various non-stoichiometric layered perovskite oxides A_2BO_4 ($A_2BO_{4\pm\delta}$) can be modified. Some oxygen excess and oxygen deficient A_2BO_4 structures are discussed in following sections.

1.7.1 Oxygen excess $A_2BO_{4+\delta}$ phases

The n = 1, RP phase based A_2BO_4 oxides consist of alternative stack of perovskite (ABO_3) and rock salt (AO) layers. These types of structures are formed a tetragonal crystal structure under symmetry group (I4/mmm space group) when t is close to unity (Figure 1.3). For t < 1 Orthorhombic and even monoclinic distortions are observed in this phases [77]. An important feature of this structure is the ability to accommodate the excess of oxygen between adjacent rock salt layers, whereby excess ions are tetrahedrally coordinated by A ions (Figure 1.3). The excess negative charge introduced by excess oxygen is neutralized by oxidation of B ions. This effect has been regarded as a way to relieve the internal lattice stresses associated with t < 1 structures [99] (in addition to rotation of BO_6 octahedra). The value of tolerance factor calculated by Eq. (1.2) using ionic radii of constituent elements is found to be t < 1 for La_2CoO_4, La_2NiO_4 and La_2CuO_4 [77]. In the absence of interstitial oxygen these compounds are orthorhombic at room temperature as a result of cooperative rotation of MO_6 polyhedral. Interstitial oxygen is introduced in La_2NiO_4 by sintering the samples in air [100]. In La_2CuO_4, the interstitial oxygen is incorporated into to the lattice by applying a pressure of 3 kbar [101], which spontaneously oxidized in air and resulting a oxygen-excess phases, e.g. $La_2CoO_{4.16}$ [102]. A tetragonal symmetry has been suggested for oxygen-excess phases $La_2NiO_{4+\delta}$, a higher value of δ is observed in the single crystal form of $La_2NiO_{4+\delta}$ like $La_2NiO_{4.13}$ [103]. The value of δ in polycrystalline phase of $La_2NiO_{4+\delta}$, δ is found to be greater than 0.14. Considering the fact that the thermal expansion coefficient of A–O (La-O) is generally larger than that of B–O (Ni-O), then the value of t would be increased with temperature and expected to be approach t ≈ 1 at their given sintering temperature [99]. For $La_2NiO_{4+\delta}$, the compound is expected to be adopted as tetragonal symmetry irrespective of oxygen stoichiometry and shows a

transition from orthorhombic to tetragonal symmetry is reported for stoichiometric phase of La_2NiO_4 at 500 °C [104]. Thermogravimetric studies of $La_2NiO_{4+\delta}$ have shown that the excess oxygen accommodated in their structure is started to leave the lattice at about 350 ºC and the process is reversible [105]. Different degrees of oxygen hyper-stoichiometry have been assigned for $La_2NiO_{4+\delta}$, which are generally reduced under strontium doping where the tetragonal symmetry is retained [103]. According to Jorgensen et al. the interstitial oxygen in $La_2NiO_{4+\delta}$ is located at (0.25, 0.25, ~ 0.23) site in the orthorhombic structure $Fmmm$ which allows interstitial oxygen to be tetrahedrally coordinated by four La atoms, but requires four neighbouring (apical) oxygen atoms to be displaced ~ 0.5 Å from their normal lattice sites [100]. However, Heaney et al. modelled the incorporation of the excess oxygen as substitution of a non-bonded O-O for apical oxygen [106].

The study on oxygen ion transport in oxygen excess RP oxides were focused on $La_2NiO_{4+\delta}$, suggests accommodation of excess oxygen in it via incorporation of oxygen interstitials in lattice [107]. As structural features of RP oxides, it made up of stacking sequence of A_2O_2 and BO_2 layers. $La_2NiO_{4+\delta}$ is a polar material which have formed an electric field gradient in between the layers of $La_2O_2^{2+}$ and NiO_2^{2-}. The coulomb potential results an anticipated large anisotropy in the transport of oxygen by preventing their interstitial sites [75]. It is well known that oxygen diffusion along a, b planes is much faster than the c-direction [89]. Using atomistic simulation calculations, Minervini et al. reported that the intrinsic disorder for $La_2NiO_{4+\delta}$ is anion frankel disorder with the oxygen vacancy situated on the equatorial site [108]. The oxygen ion migrated via an interstitial site or push - pull mechanism in which the oxygen atom located at an apical site was moved to the interstitial sites in the rock salt layer and leaves the oxygen vacancy. The creation of Frankel anion defects, which are interstitial

oxygen and oxygen vacancy, results additional oxygen content. Later calculation by Cleave et al. showed that most energetically favourable mechanism for oxygen migration in $La_2NiO_{4+\delta}$, is the movement of oxygen vacancies along a-b plane, where the equatorial oxygen vacancies are prone to migrate along the equatorial plane [75, 108, 109]. Frayret et al. have demonstrated an interstitial oxygen diffusion mechanism in $La_2NiO_{4+\delta}$ using density functional theory (DFT). They proposed that charge transfer phenomena play a major role in the oxygen vacancy migration process in which the equatorial oxygen vacancies are more favourable than apical oxygen vacancies to form Frankel ion defect [90]. The recent molecular dynamics studies (MD) shows that transport of oxygen migration takes place more favourable from apical oxygen site by interstitialcy mechanism.

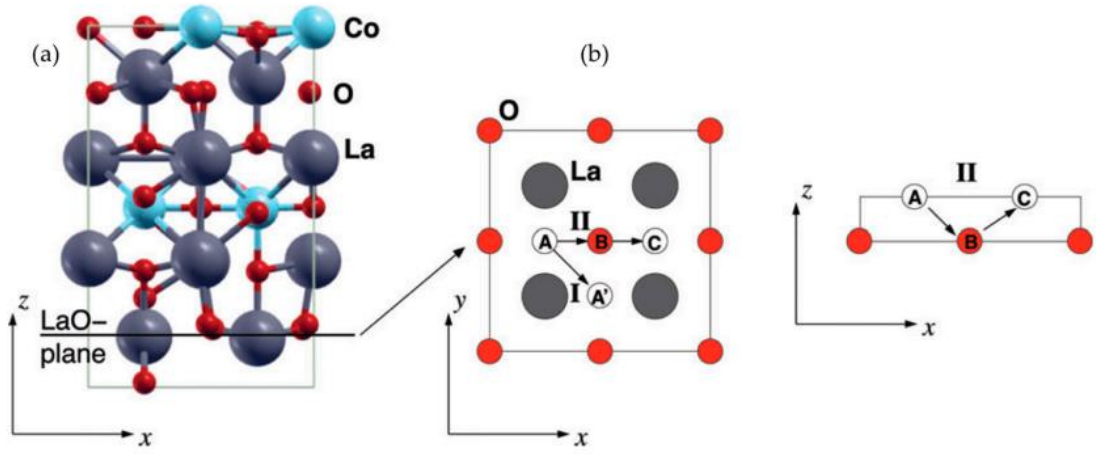

Figure 1.4 (a) Relaxed configuration of the $La_2CoO_{4+\delta}$ model. Circled region represents an interstitial oxygen atom; and **(b)** migration paths in simulation. (I) indicates an interstitial migration (II) shows an interstitialcy migration mechanism [75].

The MD simulations of $Pr_2NiO_{4+\delta}$ indicated that oxygen ion migration in $Pr_2NiO_{4+\delta}$ is highly anisotropic which occurred via interstitial mechanism is well explained by Prafitter et al. [110]. Further it is also reported that the degree of excess oxygen strongly influenced the activation energy for oxygen migration. Similar to $La_2NiO_{4+\delta}$, the

calculation done for $La_2CoO_{4+\delta}$ showed that oxygen vacancies at equatorial sites are more favourable for migration in the equatorial plane as compared to interstitial sites by Allan et al. [75]. The calculated results of oxygen vacancies migrates dominantly via an interstitial sites in $La_2CoO_{4+\delta}$, by Kushima et al. [111] was shown in Figure 1.4. Both calculations DFT and MD demonstrated that the activation energy required for oxygen migration via interstitial site was lower than the activation energy required for direct interstitial exchange site is proposed.

1.7.2 Oxygen deficient $A_2BO_{4-\delta}$ phases

In oxygen deficient phase $A_2BO_{4-\delta}$, there are two oxygen sites is present as depicted in Figure 1.3 by O1 and O2. The oxygen deficiency is often produced within the equatorial planes of BO_2 i.e., O1 sites of the structure along equatorial direction and O2 along apical direction. By reduction of the stoichiometric in A_2BO_4 phases, the oxygen deficiency is produced in these materials. However for $NdSrCuO_{4-\delta}$, a distribution of oxygen vacancy between apical and equatorial sites has been reported [112]. On the other hand, oxygen vacancies may order or disorder within the equatorial planes of the structure. A distribution of vacancy order within the BO_2 planes was occurred similar to $Ca_2MnO_{3.5}$ [113]. The material is therefore formed of sheets of five-coordinate cations with square pyramidal coordination. A different pattern of MnO_5 square pyramids interconnected in these sheets has been suggested by Greaves et al. for $Sr_2MnO_{3.5}$ shown in Figure 1.5 [114]. Reduction studies on $La_{2-x}Sr_xNiO_{4-\delta}$ phases showed that the vacancy in the Ni-containing materials $La_{1.6}Sr_{0.4}NiO_{3.47}$ and $LaSrNiO_{3.1}$ is confined to the equatorial planes with strong preference to occur along one of the tetragonal axes of the K_2NiF_4 structure [115]. More recent studies on the reduction of $LaSrCoO_4$ using hydrogen and sodium hydride allowed the isolation of reduced phases with the composition $LaSrCoO_{3.5-x}$ [116]. Oxygen vacancies in these materials are disordered

and confined to the equatorial BO_2 planes of the structure. This type of vacancy does not affect the lowering symmetry and tetragonal symmetry and the parent compound ($I4/mmm$ space group) was retained to same crystal strcuture.

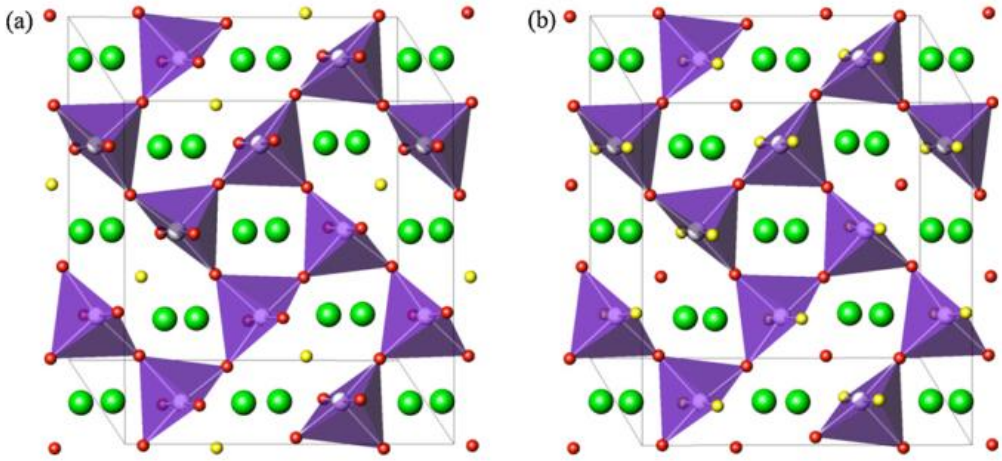

Figure 1.5 (a) Crystal structure of $Sr_2MnO_{3.5}$ with equatorial oxygen vacancies along bc plane **(b)** Crystal structure of $Sr_2MnO_{3.5}$ with atoms displacing oxygen atoms from their apical positions thus causing the oxygen atoms to fill the equatorial vacancies, such that the fluorinated material reverts to I4/mmm symmetry (green- Sr, white-Mn, red- O, yellow-vacant site) [114].

Further, the addition of acceptors in A_2BO_4 based RP oxides makes it a oxygen deficient RP oxides [75]. Consider La_2NiO_4 is the host and Sr used as substituent for La-site then the overall materials exhibit the oxygen deficiency due to this substitution. Opila et al. proposed a defect model for Sr-doped cuperates ($La_{2-x}Sr_xCuO_{4-\delta}$), showing anisotropic oxygen transport properties [117].

$$2SrO \xrightarrow{La_2CuO_4} 2Sr_{La}{}' + V_{\ddot{O}} + 6O_o{}^x \qquad (1.12)$$

The overall electroneutrality for above Eq. (1.12) can be understood by following way;

$$p + 2[V_o^{\cdot\cdot}] = n + 2[O_i''] + [Sr_{La}{}'] \qquad (1.13)$$

Opila et al. further suggested that the oxygen vacancy migration in $La_{2-x}Sr_xCuO_{4-\delta}$ is takes place for the lower concentration of Sr ($x<0.07$) [117]. Mazo et al. demonstrated a MD simulation on $La_{2-x}Sr_xCuO_{4-\delta}$ and reported the presence of small anisotropy in crystal structure of $La_{2-x}Sr_xCuO_{4-\delta}$ which leads to various oxygen transport properties in (La,Sr)O blocks and CuO_2 layers. The conventional oxygen vacancy migration mechanism is more favourable for composition with $x>0.07$ [118].

Sawin et al. performed the MD simulation on oxygen migration mechanism and they proposed that the oxygen migration is mainly occur in CuO_2 layers with the help of hopping mechanism [119]. In addition they also pointed out that although the energy required for migration of oxygen vacancies along the apical site was lower than that of the equatorial site. The oxygen vacancy migration with great diffusivity occurred along the c-direction. As the vacancies present at the apical sites must pass to the equatorial site then it results increase in the activation energy [75]. The oxide ion migration mechanism of $La_{2-x}Sr_xCuO_{4-\delta}$ for high Sr levels ($x=0.8$-1.2) were reported by MD simulations (Figure 1.6). They proposed that oxygen diffusion in oxygen deficient phase $La_{2-x}Sr_xCuO_{4-\delta}$ is mainly attributed to the migration of oxygen vacancies within the perovskite layer, whereas an interstitialcy mechanism is dominant for oxygen excess $La_{2-x}Sr_xCuO_{4+\delta}$ phase. They further suggested that it is also possible for oxygen vacancies to migrate through long range paths between adjacent layers.

Schroeder et al. investigated that the oxygen transport property of polycrystalline $La_{2-x}Sr_xNiO_{4-\delta}$ samples experimentally that the oxygen migration upto $x=0.5$ is mediated mainly by interstitial oxygen which was occurring parallel to the layers of the structure [120]. The contribution of vacancy migration could not be ruled out due to their lower concentrations present in the samples.

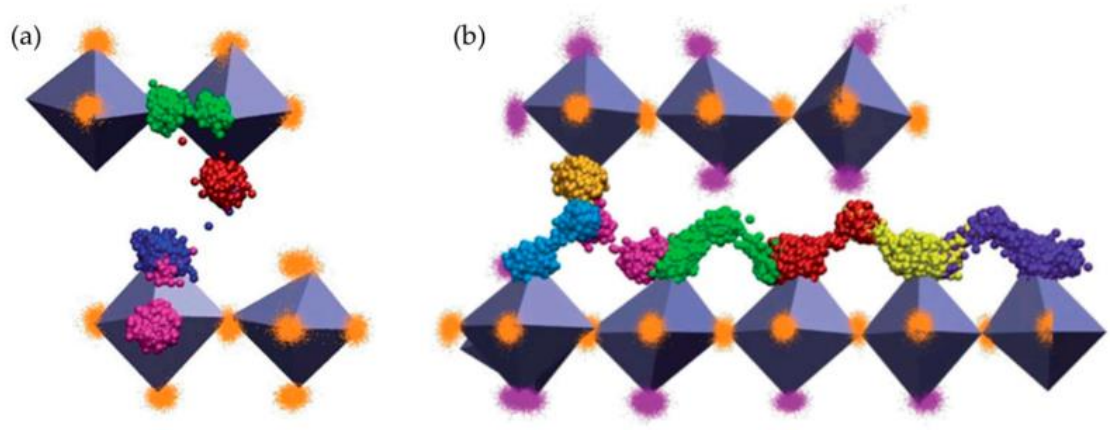

Figure 1.6 (a) 3D representation of oxygen vacancy migration within the CoO6 octahedron (pink and red), between the equatorial and the apical (green and blue) positions in $La_{0.8}Sr_{1.2}CoO_{3.9}$; **(b)** 3D representation of oxygen interstitial migration in $La_{1.2}Sr_{0.8}CoO_{4.1}$. Each oxygen involved in the migration event is represented by a different color. Spheres of the same color indicate the positions occupied by a specific atom over the simulation time [75].

1.8 Properties of A_2BO_4 oxides

Based on the existence structure of A_2BO_4, either in oxygen deficient or oxygen efficient type structures are found. As already discussed in the preceding section, the charge compensation mechanisms on incorporation of oxygen interstitial as well as oxygen loss and also via chemical substitution, the variety of properties are studied. In oxide ceramics, the key role factor is the oxygen non-stoichiometry and the presence of multivalent ion. These two factors are manipulated by various ways and modified the properties orientated towards variety of applications. In following sections the properties of A_2BO_4 type oxide materials are described.

1.8.1 Electrical Properties

The RP oxide phases were described in terms of oxygen deficient and oxygen excess phases. Based on the different kinds of doping, the properties of RP oxides are modified

for various electrical device applications. Rare earth based nickelates (La_2NiO_4) is the widest studied materials for the possible application in cathode as well as anode in solid oxide fuel cell (SOFCs). The electrochemical performance of SOFCs is strongly dependent on the catalytic activity of cathode materials which involves the oxygen reduction reaction (ORR) due to slow oxygen reduction kinetics at reduced temperatures [121]. Therefore, it is a major challenge to explore efficient and high-performance cathode materials for oxygen electrocatalysis in order to accelerate ORR kinetics, from which the detailed mechanism of mixed ionic-electronic cathode materials can be effectively understood. The oxygen reaction pathways on mixed ionic-electronic conducting cathode materials are the gas diffusion, adsorption, dissociation, surface diffusion, bulk diffusion, charge transfer process, ion transfer at three phase boundary (TPB), and the catalytic activity is mainly determined by controlling the rate of one of several oxygen transport processes [122] are used to understand oxygen diffusion coefficient (D) and surface exchange coefficient (k) in mixed ionic-electronic conductors. The pulse isotope ^{18}O-^{16}O exchanged (PIE) rapidly measures the oxygen surface exchange of mixed ionic-electronic conductors which provided a new insight into the mechanism of oxygen surface exchange process [123]. As typical cost-effective cathode materials, the RP oxides with a general formula of $A_{n+1}B_nO_{3n+1}$ have used in large oxygen storage capacity and mixed ionic-electronic conductivity [124]. The layered perovskites Pr_2NiO_4, La_2NiO_4, and La_2CuO_4 show excess oxygen compositions and the interstitial oxygen easily migrated along the rock salt layer, providing high anisotropic oxygen-ion conduction which was used as an oxygen ion conductor in electrochemical devices [75].

Similarly, two-perovskite-layer oxide, $Sr_3Fe_2O_{7-\delta}$ with two perovskite $SrFeO_{3-\delta}$ and SrO rock salt structures alternately stacked, which were used in large oxygen storage

capacity, water-intercalation capacity and excellent catalytic activity [125]. Unlike interstitial oxygen formation in single-perovskite-layer oxides, the majority of oxygen vacancies in $Sr_3Fe_2O_{7-\delta}$ are preferentially located at the oxygen site between two FeO_6 octahedrons along c axis. The anisotropy of the conduction of charge carrier in $Sr_3Fe_2O_{7-\delta}$ makes it used in application of thin film memory devices [126].

The n=∞ member of the $Sr_{n+1}Ti_nO_{3n+1}$ Ruddlesden Popper homologous series, $SrTiO_3$, exhibits a wide range of electrical behaviour: from a high dielectric constant tuneable paraelectric in its undoped form, to a metallic superconductor when doped with a variety of elements. It has been studied as a substrate for perovskite oxides and for application in tunable dielectric devices, dynamic random access memory and as an alternative gate oxide in metal–oxide–semiconductor field effect transistors~ (MOSFETs). For example, polycrystalline samples of Sr_2TiO_4 (n=1) and $Sr_3Ti_2O_7$ (n=2) exhibit lower dielectric loss than $SrTiO_3$. $SrTiO_3$ is the only member of the series that melts congruently [120, 121].

However, the dielectric properties of the Ruddlesden Popper oxides were shown a high value of dielectric constant with low value of dissipation factor which is commonly found in giant dielectric materials. The high dielectric constant materials can be used in multilayer chip capacitors, tunable devices, and random access memory devices etc. [127]. Dielectric properties of the nanosheets of perovskite and layered perovskite have been shown reasonable improvement by changing in their composition and structure of layered perovskite materials [129]. The dielectric constant of layered perovskite materials has been reported that it could be affected by the number of octahedral layers and polarizability of material which plays a crucial role in the dielectric properties of materials. However, the polarizability of octahedral layers can be controlled by varying the A-site, B-site or both independently or by co-doping at the same time [127]. The

dielectric properties of homologous series of $Sr_{n+1}Ti_nO_{3n+1}$ were found to be increasing with n, for example the dielectric constant of n=1 member was lower than n=2 and highest for n=∞ i.e., $SrTiO_3$ [127–129].

1.8.2 Magnetic Properties

The electronic properties of Fe^{4+} in ternary oxide are rather complex with small changes in composition and oxidation states, markedly affect the electron distribution. Recently, we have described the synthesis of the stoichiometric Fe^{4+} oxides Sr_2FeO_4 and $Sr_3Fe_2O_7$ by reaction of the component oxides under high-pressure oxygen and determined their structures at room temperature by powder X-ray and neutron diffraction [130]. Sr_2FeO_4 crystallises with the K_2NiF_4 structure [Figure 1.2] with an almost regular octahedral coordination to iron in Sr_2FeO_4, can be considered as a Ruddlesden-Popper phase with a 1:1 intergrowth of Sr_2FeO_4 and perovskite $SrFeO_3$. Sr_2FeO_4 orders antiferromagnetically at 60 K whilst the Nee1 temperature of $Sr_3Fe_2O_7$ is 110 K. At room temperature, the Mossbauer spectrum of $Sr_3Fe_2O_7$ is interpreted in terms of a disproportionation, $2Fe^{4+} \rightarrow Fe^{3+} + Fe^{5+}$, though neutron diffraction measurements show the presence of single crystallographic iron site. Neutron diffraction data collected below the Nee1 temperatures from Sr_2FeO_4 (4 K) and $Sr_3Fe_2O_7$ (6 and 90 K) only show broad weak magnetic reflections indicative of antiferromagnetic ordering in two dimensions. Mossbauer data collected below T_N from Sr_2FeO_4 indicates the presence of at least four magnetically different Fe^{4+} sites [79].

A large negative magnetoresistance (MR) effect at low temperatures (45% at 5 K and 9 T) has been observed for the iron (IV) - based Ruddlesden–Popper type phase $Sr_3Fe_{1.8}Co_{0.2}O_7$. Measurements of magnetic sensitivity and isothermic magnetization suggest a cluster - glass magnetism with strong ferromagnetic and competing

antiferromagnetic interactions. This semiconducting material's properties are closely correlated with magnetic and magnetoresistance. The magneto transport behaviour of $Sr_3Fe_{1.8}Co_{0.2}O_7$ is interpreted as covalence — driven electron transfer processes between the orbitals of adjacent metal ions that stabilize the ferromagnetic alignment of the more localized t2 g electrons [79, 130].

1.8.3 Optical Properties

The development of flat-panel displays including field emission displays (FEDs), plasma display panels (PDPs) and thin film electroluminescent devices (TFELs) were accompanied by improvements in the phosphors used in this application. There has been a lot of effort to discover new host materials and high-performance activators for phosphorus applications [131]. Oxide phosphors are more attractive than the traditional sulphide or halide phosphors due to their high resistance in nature from a practical point of view. Alkaline earth ortho-stannates (M_2SnO_4, where M = Ca, Sr and Ba) have been found as a host matrix for new phosphors because of their stable crystalline structure and high physical and chemical stability [131]. The incorporation of optically active lanthanide ions into the host matrix of orthostannate resulted in phosphors with photoluminescence (PL) [132] and long lasting phosphorescence (LLP) properties [133]. The performance of LLP phosphors emitting in the blue and green spectral region almost meet the requirement for practical applications are commercially widely available in optical devices [124,127]. However, orange to red LLP phosphors are still out of reach from a practical point of view. Therefore, there is still a strong need for the development of novel host materials for LLP phosphors emitting at longer, i.e. in the wavelength range orange to red [134]. In general, the properties of LLP phosphors can be adjusted by using a host-mixing method to change the original constituents of the lattice or introducing different co-dopant [127,128]. Important performance factors of

the phosphor materials are the band gap, the energetic distance of the excited state to the conduction band and the type and energetic location of defects present which played a vital role in enhancement of luminescence application. The luminous colour parameters of the white LED are also important factor for the applications in white LED and they depend on the emission centres of the phosphors. The red and orange emission of phosphor mainly derives from the electron transition of the internal orbit of Sm^{3+} and Eu^{3+}. The Sm^{3+} (electron configuration $4f^5$) and Eu^{3+}(electron configuration $4f^6$) ions have many energy levels and incomplete 4f shell and their outer $5s^2$ and $5p^6$ orbits shield 4f against the crystal field [124, 125, 129]. Therefore, the optical spectra of Sm^{3+} and Eu^{3+} in crystal lattice are fairly similar to the free ions and show the good colour purity. The purple photochromism by Eu^{3+} doping in Sr_2SnO_4 by varying temperature and time of reaction reported by Kamimura et al. [137]. The incorporation of Ti^{4+} in many alkaline earth orthostannates (A_2SnO_4: A=Ca, Sr, Ba) has studied as blue photoluminescence applications. According to Kazushige Ueda et al., the excitation spectrum of these stannates exhibited broad bands just below the fundamental absorption edges, implying that the luminescence centres did not consist of the host material components. It is suggested that the isolated TiO_6 complexes are possible luminescence centres in these materials, as previously proposed in other Ti-doped stannates such as Mg_2SnO_4 and $Y_2Sn_2O_7$ [138].

1.9 Objectives of the work

The layered perovskites were first studied by S.N. Ruddlesden and P. Popper in 1958 hence they are known as RP oxides. RP oxides have shown attractive and versatile physical properties such as superconductivity, magnetoresistance, and mixed ionic and electronic conductivity, which are potential candidates for energy and electronic devices. The Ruddlesden Popper oxides are represented by general formula

$A_{n+1}B_nO_{3n+1}$, where n is a positive integer, for example n=1 A_2BO_4, n=2 $A_3B_2O_7$ and so on. The structure of the first member (n = 1) of this series, A_2BO_4 which is formed as K_2NiF_4 type structure. The A_2BO_4 is built of an alternate stacking of a perovskite slab (ABO_3) and a rock-salt slab (AO). In A_2BO_4 structure, the A ion is coordinated by nine oxygen ions and the B ion is coordinated with six oxygen ions. The unit cell is tetragonal having I4/mmm symmetry with lattice parameters are a=3.9 Å and c ~ 3a Å. To obtain this structure, the ratio of the radius for A and B ions r_A/r_B should be lie in the range of 1.7 to 2.4.

In general ABO_3 oxides are found as oxygen-deficient perovskites, whereas A_2BO_4 oxides can be found as both oxygen-deficient and oxygen-excess, depending upon their majority of oxygen defects. In A_2BO_4 system, excess oxygen can be accommodated in the AO layers are formed as an interstitial oxygen defect. Hence, oxygen ion migration in A_2BO_4 oxides can occur via mechanisms associated with either oxygen vacancies or oxygen interstitials. Further atomic packing fraction of perovskite oxides is higher than that of these layered perovskites.

In Sr_2SnO_4 structure, SnO_6 octahedra are linked by sharing edges with each other and two-dimensional perovskite-like layers. In this kind of low-dimensional structure, it is easy to implant of ions as doping into the host lattice and hence manipulate its physical and chemical properties. Substituents of La, Nd and Eu at A and B sites of perovskite oxides ABO_3 (A=Ca, Sr, Ba and B=Ti, Sn) have exhibited significant improvement in their physical properties. Based on the modified properties of these oxides, many technological applications of these oxides have been explored.

Development of new materials with improved properties is the need of present and future requirements of the society. In view of above-mentioned results, in this work

for the first time few single phase solid solutions have been synthesized. Effects of selected dopants on the properties of Sr_2SnO_4 have been studied in detail. Further, it is worth mentioning here that to study explicitly role of the dopant, processing parameters (calcination and sintering temperature and time) are kept same for all the samples. Systems, compositions and properties investigated in this work are presented below;

System	Compositions	Code	Properties
Sr_2SnO_4	--------	--	Structural, Optical, and Electrical properties.
$Sr_{2-x}Ba_xSnO_4$	Sr_2SnO_4 (x=0.00)	SSB0	Structural, Dielectric and Electrical properties.
	$Sr_{1.80}Ba_{0.20}SnO_4$ (x=0.20)	SSB1	
	$Sr_{1.60}Ba_{0.40}SnO_4$ (x=0.40)	SSB2	
	$Sr_{1.20}Ba_{0.80}SnO_4$ (x=0.80)	SSB4	
	$Sr_{0.40}Ba_{1.60}SnO_4$ (x=1.60)	SSB8	
	Ba_2SnO_4 (x=2.00)	SSB10	
$Sr_{2-x}La_xSnO_4$	Sr_2SnO_4 (x=0.00)	SSL0	Structural and Electrical Properties.
	$Sr_{1.99}La_{0.01}SnO_4$ (x=0.01)	SSL1	
	$Sr_{1.98}La_{0.02}SnO_4$ (x=0.02)	SSL2	
	$Sr_{1.96}La_{0.04}SnO_4$ (x=0.04)	SSL4	
	$Sr_{1.94}La_{0.06}SnO_4$ (x=0.06)	SSL6	
	$Sr_{1.90}La_{0.10}SnO_4$ (x=0.10)	SSL10	
$Sr_{2-x}Nd_xSnO_4$	Sr_2SnO_4 (x=0.00)	SSN0	Structural and Magnetic Properties.
	$Sr_{1.99}Nd_{0.01}SnO_4$ (x=0.01)	SSN1	
	$Sr_{1.98}Nd_{0.02}SnO_4$ (x=0.02)	SSN2	
	$Sr_{1.96}Nd_{0.04}SnO_4$ (x=0.04)	SSN4	
	$Sr_{1.94}Nd_{0.06}SnO_4$ (x=0.06)	SSN6	
	$Sr_{1.90}Nd_{0.10}SnO_4$ (x=0.10)	SSN10	
$Sr_2Sn_{1-x}Eu_xO_4$	Sr_2SnO_4 (x=0.00)	SSE0	Structural and Optical Properties
	$Sr_2Sn_{0.99}Eu_{0.01}O_4$ (x=0.01)	SSE1	
	$Sr_2Sn_{0.98}Eu_{0.02}O_4$ (x=0.02)	SSE2	
	$Sr_2Sn_{0.96}Eu_{0.04}O_4$ (x=0.04)	SSE4	
	$Sr_2Sn_{0.94}Eu_{0.06}O_4$ (x=0.06)	SSE6	
	$Sr_2Sn_{0.90}u_{0.10}O_4$ (x=0.10)	SSE10	

Note- Concentration of hetrovalent substituents (La, Nd and Eu) is kept low ($x \leq 0.10$) to achieve single phase solid solutions.